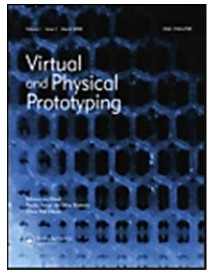

Pilot study describing the design process of an oil sump for a competition vehicle by combining Additive Manufacturing and carbon fibre layers

Journal:	*Virtual and Physical Prototyping*
Manuscript ID:	NVPP-2015-0017.R1
Manuscript Type:	Review
Keywords:	Composite panel, Fused deposition modelling (FDM), Computer-aided engineering, Rapid manufacturing

Pilot study describing the design process of an oil sump for a competition vehicle by combining Additive Manufacturing and carbon fibre layers

Abstract:

Formula Student is an international competition governed by the Society of Automotive Engineers (SAE) that challenges university students to design and build a racing car that will subsequently be compared against other cars from universities around the world in homologated racing circuits by non-professional drivers. This study focuses on the design, analysis and manufacturing process of a new oil sump for a Formula Student car —by combining a main ABS-plastic core as a result of an additive manufacturing printing process and a later manual lay-up process with carbon fibre— in order to reduce the sloshing effect due to the movement of the oil while racing.

The new oil sump and the original sump were modelled in a Computer-Aided Design software and five CFD simulations were performed to compare the sloshing effect in both designs in three driving scenarios: acceleration, braking and changes in direction. Simulations show that acceleration is not a critical situation since the new internal design of the sump was capable of delaying immersion time of the oil pick-up pipe from 0.75 seconds to 2 seconds during braking and from 0.4 seconds to 0.8 seconds during a lateral acceleration.

The new design was physically manufactured and subsequently assembled on an internal combustion engine for testing for 45 minutes. During this test, the engine was started and put at 9600 RPM, so the oil worked under realistic temperature conditions (80ºC). It did not present any oil leak. After testing, it was disassembled and visually inspected. No failure in the inner surfaces of the oil sump was observed due to temperature.

According to these results, the present research argues that the combination of an additive manufacturing technology (i.e. Fused Deposition Modelling) and layers of carbon fibre is a real alternative to conventional manufacturing processes with which getting geometrically complex oil sumps that minimize the sloshing effect in competition automobiles.

Keywords: Oil sump, Additive Manufacturing, Fused Deposition Modelling, ABS plastic, Carbon fibre, Computational Fluid Dynamics

Introduction

The Formula Student (FS) competition challenges teams of university undergraduate and graduate students to conceive, design, fabricate and compete with small, formula style vehicles (SAE International 2013). The FS regulation for the electric and the internal combustion engine cars establish very few technical requirements that the designed car has to meet and they put special emphasis on the team's self-sufficiency, innovation and creativity when designing and manufacturing any component of the car. With this in mind, one of the most challenging issues that engineers must face in competition vehicles, and in the automotive industry in general, is weight reduction; this is usually done by replacing heavier ferrous and non-ferrous metals with lighter metals, polymers or composites. Although in regular automobiles the goal of reducing weight is primarily to improve fuel efficiency and reduce CO2 emissions, competition vehicles seek to reduce lap time. Among the different available technological options, Additive Manufacturing (AM) is becoming in a real solution for replacing a car's main components by weight-optimised parts since it allows almost any virtually designed geometry to be created. AM can be defined as the process of joining materials to make objects from 3D model data, usually layer upon layer, as opposed to subtractive manufacturing methodologies (American Society for Testing and Materials International 2012). Its main advantage with respect to traditional manufacturing methods is that virtually any geometry can be built, offering almost unlimited and unconstrained geometric complexity. In essence, the statement 'What You See Is What You Build (WYSIWYB)' can often be achieved (Gibson et al. 2010). Using the available AM technologies, FS teams have worked on the design and analysis of some of the car's main components. These components are made of plastic or metallic alloys and enclose parts such as the steering knuckle (Elsevier Ltd 2013), the brackets connecting the suspension and the chassis(Spierings et al. 2011), the accelerator pedal arm(Prada et al. 2015), the body and side pods for the Areion car developed by Group T team or the heat transfer component (Neugebauer et al. 2001).

With respect to the use of AM technologies and carbon fibre in FS cars, two references were found in the literature, and both of them were related to the engine intake runner but used different AM technologies. In the first one, the team from École Polytechnique de Montréal (Canada) developed and manufactured a new design using Selective Laser Sintering (SLS) and a new material code named Nytek 1200 CF, which is a polymer (Nylon12) filled with carbon fibres (Black 2010). In the second one, Ilardo and Williams(2010) created a functional intake manifold for a FS car using an additive manufactured part printed with Fused Deposition Modelling (FDM) technology that was later covered in layers with carbon fibre composite. Both designs were capable of withstanding high temperatures and pressures with no signs of failure during the testing phase. Following this last approach, the present paper deals with another critical component that has the potential to combine the design freedom that additive manufacturing technologies provide and the structural strength that carbon fibres give: the oil sump of an internal combustion engine.

The oil sump, along with the pressure pump and the oil filter, are the main components of the lubrication system of an automobile. It is also called a wet sump system since the sump is used as the main oil reservoir. The opposite system is the dry sump system, where an external reservoir stores the oil while the oil sump is only employed to collect the fallen oil with the help of a scavenge pump which transfers it back to the external reservoir. Sumps in commercial vehicles are usually made of metallic alloys that are normally based on steel or aluminium, common polymers or composite materials (i.e. polyamide with glass fibre), and they are manufactured via CNC machining, forming, casting or injection moulding in case of plastics. Among the two systems, dry systems are preferred in racing cars as they enhance vehicle performance: the vertical dimension is reduced, the engine can be placed closer to the ground and, as a consequence, the centre of gravity is lower and the corner speed is better. However, dry systems, in contrast to wet systems, tends to increase any lubrication issue related to large acceleration forces that can pull the oil away from the pick-up pipe of the pump, an issue known as sloshing.

Sloshing is the term that defines the movement of a liquid free surface due to external disturbances. Liquid sloshing has been widely studied in partially filled moving containers since the 1960s (Abramson 1966), and it is directly related to the external excitation applied by the driver, such as braking and accelerating. Assuming an incompressible liquid having no viscosity, the fluid motion within the tank is described by reducing Navier–Stokes equations to Euler equations. When severe sloshing is considered, full Navier-Stokes equations are calculated using computational methods such as the CFD (Computational Fluid Dynamic) commercial software ANSYS Fluent, which is based on finite volume discretization. Simulations for liquid sloshing are calculated by considering either laminar or turbulent flows in a variety of situations: Liquefied Natural Gas (LNG) tanks, containers filled with water, etc. (Godderidge et al. 2006; Godderidge et al. 2009; Lee et al. 2011; Rhee 2005). In order to avoid sloshing, containers incorporate internal baffles whose placement, shape and material is variable. The effect of baffles has been investigated in tank trucks through experimentation and virtual analyses by considering both rigid and flexible baffles (Dodge 1971; Stephens and Scholl 1967). "Similarly, automobiles ensure the continuous supply of oil to the pressure pump by using sumps that have complex geometries and internal baffles, which are made of aluminium or steel and welded to the main body of the sump after it has been manufactured.

This study explores the possibility of manufacturing an end-use oil sump for a Formula Student car that presents a reasonable level of performance with respect to the existing aluminium sump and follows the spirit of seeking to improve performance through innovation and creativity. The manufacturing process combines AM and carbon fibre and to the best of authors' knowledge, this is the first time that the methodology for obtaining an AM oil sump covered with carbon fibre for a racing vehicle is reported. To achieve that goal, a complete process of design, analysis and manufacturing is described: both the original and the new oil sump were designed within a CAD application and prepared in terms of constraints for Computational Fluid Dynamic (CFD) analyses. Subsequently, the physical prototype of the new design was manufactured using a relatively low-cost Fused Deposition Modelling (FDM) AM technology and then layered with carbon fibre.

Finally, this physical prototype was assembled on an internal combustion engine and tested under nominal working conditions in terms of temperatures to verify the suitability of the novel manufacturing approach. All this work was done following the Formula Student spirit of in-house design and manufacturing.

Methods

Modelling

Our FS car has the engine of a Suzuki GSRX 600 motorcycle. The original oil sump from this engine, which was mounted on the FS 2012 car, was replaced by an improved version that included several geometry changes in order to increase the performance of the FS 2013 car (Figure 1). These changes included a lower height and new V-shaped baffles surrounding the oil pick-up pipe, which is placed in a region opposite the acceleration direction of the car. The sump is made of aluminium and weights 604 grams, and it is attached to the engine body by means of 14 screws placed along the perimeter. The sump of the FS 2013 car was modelled in SolidWorks (Dassault Systemes, Velizy Villacoublay, France) and manufactured with an in-house CNC centre. The manufacturing process required 24 hours of labour to prepare the CAM program and 6 hours of machining in the CNC-centre. The total cost of the manufacture, including labour, is estimated to be above 1500€. Despite these changes, the design was not yet optimum since the drivers could feel that the engine suffered from lack of lubrication: the pick-up pipe was not completely submerged in oil. This feedback was confirmed by serious breakdowns of the engine. Identified as a critical issue that drastically threatened the life of the engine, the decision was made to redesign again the sump for the upcoming FS cars in order to solve this issue by means of a more complex baffle geometry. However, the shape of the new baffles could not be limited by the available chip removal manufacturing process (milling or drilling).

The targets of weight reduction and a more complex baffle geometry motivated a new sump design for the new FS vehicle using AM technologies, which allows virtually any geometry to be reproduced in lightweight materials, and carbon fibre lay-up in order to increase the part stiffness with no weight penalization. Thus, the new design was modelled in CREO 2.0 (PTC, Needham, MA, USA) and included complex wave-shape baffles which are very hard to fabricate with conventional techniques. The final lay-up process was considered during the design stage: hence, the oil sump was simplified at its perimeter by removing some curved surfaces and replacing them with planar surfaces. In this way, the later lay-up process with carbon fibre was simplified. The positioning of the 14 holes remained identical. The average thickness at the bottom region is 3 mm. (Figure 2).

CFD simulation

The two designs were computationally compared in order to analyse the baffle performance under multiple movement scenarios via Computational Fluid Dynamic (CFD) analysis.

The sloshing model was developed in ANSYS Fluent code, version 14.5 (Canonsburg, Pennsylvania, USA) and was a nonlinear model that used the Finite Volume Method to integrate the Navier-Stokes equations. The multiphase model to track air-oil interface is the Volume-of-Fluid (VOF) method of Hirt and Nichols (1981), which assumes a fixed mesh in the domain and both fluids as incompressible immiscible fluids. The VOF method calculates free surface position via volume fraction. The flow regime is assumed to be laminar and no turbulence models were implemented. The oil had a density of 889 kg/m3 and a viscosity of 1.06 kg/m-s while the air had a density of 1.225 kg/m3 and a viscosity of 1.7894 e-05 kg/m-s

The flow domain was created by considering the available space for the oil sloshing inside of the engine during normal conditions. Thus, the domain was constrained by the inner surfaces of the oil sump and some internal components of the engine. The surfaces of each oil sump were directly taken from the 3D CAD files while the internal components of the engine were digitised by means of the RevScan 3D laser scanner (Creaform3D, Lévis, Quebec, Canada), a non-contact hand held self-oriented scanner that consists of a laser emitter and two cameras. The laser light is projected onto the object's surface, and its reflection is captured by the two cameras, which triangulate the laser within a specified focal area (Figure 3). After scanning, the geometry was exported via Stereolithography (STL) and taken as reference in CREO in order to help model the simplified surfaces that represented the upper geometry of the flow domain for the CFD simulations. With this methodology, the old and the new design shared the upper surfaces of the flow domain, while the bottom surfaces including the baffles were those corresponding to each oil sump (Figure 4).

The body force approach is used to simulate the car's oil sump movement(Godderidge et al. 2006). Three scenarios were simulated for each oil sump by considering real tests carried out with the FS car: an acceleration of 0.5 g's for 5 seconds, a braking of 1g for 2.5 seconds and a lateral movement, which replicated a high speed corner, of 1g for 6 seconds. Apart from the corresponding movement of each scenario, a second body force was taken into account: gravity in the vertical direction. At the initial time, the fluid is at rest and the initial operating pressure is assumed equal to the atmospheric pressure.

The domain for the simulation of the old oil sump was defined with a mesh of 514,962 tetrahedral cells. It was assumed that the oil height inside the oil sump was 22 mm and corresponded to 300,891 cells. The new oil sump was defined with 428,764 tetrahedral cells. The oil height was also 22 mm and grouped 257,436 cells. The entire domain was enclosed within solid wall elements.

The Non-Iterative Time Advancement (NITA) scheme was adopted for the transient simulation, using the Fractional step method as a velocity-coupling scheme. The time step was variable but with a minimum value of 1e-07 seconds. The typical time step was around 5e-05 seconds. The first order upwind discretization scheme was used for the momentum equations while

Geo-reconstruct was used for volume fraction equations. The simulations were solved using a high-performance computing cluster with an installed capacity of 32 processors with 128 GB of RAM.

Manufacturing

For the manufacturing process, the oil sump was firstly exported to STL, and later manipulated using MAGICS v18.02 (Materialise, Leuven, Belgium). In this study, MAGICS was used to divide the oil sump in smaller parts to accommodate the 3D printer's build tray dimensions. To this end, the oil sump was cut along two partition lines in order to get the sump divided into four parts. The correct positioning of each part relative to the other parts was assured with the use of connector pins modelled within MAGICS. Subsequently, each part was built on a HP DesignJet Color 3D printer (now commercialised by Stratasys) based on FDM technology. The printer features 254-micron layers and the building material was acrylonitrile–butadiene–styrene (ABS) copolymer (P430). The necessary support material was later removed in a bath with water and sodium per carbonate. Once cleaned, the physical parts were joined together with cyanoacrylate glue (Figure 6).

Once joined, 14 metallic cylinders were inserted inside the perimeter holes to locally increase the stiffness of the region of the sump near the 14 tightening screws. This was followed by the manual wet lay-up of the composite material onto the oil sump. For the lay-up process, a 2/2 twill carbon fibre featuring a weight of 199 grams per square metre was used. A total of eight sheets, four for the inner surfaces of the oil sump and four for the outside, were layered-up, following a 90º/45/90º/45º orientation. There were two main reasons for layering-up the AM part:

- To avoid oil leakage caused by the porosity of the sump printed with FDM technology. This is the reason why carbon fibre layers with a reasonable density (199gr/m2) are used.
- To reinforce the overall oil sump structure. The oil sump is subjected in one hand to the 10Nm preload of the 14 bolts used to fasten it to the engine, but it can also suffer

impacts from any external element during the race. The benefits of carbon fibre in this sense are very well known.

The orientation of the layers was set by trying to reinforce the part in a homogeneous way, equally reinforcing all directions, as there is no critical direction in the stress solicitation of the part. Each layer was impregnated with a mix of high temperature carbon fibre skinning basecoat and hardener suitable for an end use at up to 180ºC (EasyComposites, Longton, Stoke-on-Trent, UK). Then, the oil sump was covered with a peel ply that facilitated the later demoulding process, and a cotton mat that absorbed the excess resin. The process was completed by putting the oil sump inside a vacuum bag while an external vacuum pump evacuated air from the inside of the bag. The oil sump was left under vacuum for 72 hours at ambient temperature (20ºC). The final prototype of the sump after the layering process weights 474 grams (a reduction of 21% with respect to the aluminium one) and is depicted in Figure 7.

Tensile testing

Tensile tests were performed to analyse the influence of carbon fibre layers in terms of strength with respect to the sole ABS plastic. The specimens for tensile tests were modelled in accordance with BS EN ISO 527-2:1996 as shown in Figure 8 and using CREO 2.0 CAD. The specimen was then exported to STL file format and printed using the HP 3D printer.

Test specimens were produced at a nominal thickness of 4 mm and they were printed taking different printing orientations into consideration. A total of eight specimens were printed, that is, two copies for every main printing orientation —XY, XZ, YX, and YZ— where the first letter denotes the specimen's main axis and the second letter is the minor axis (Table 1). The remaining two directions (ZX and ZY) were not considered since the specimens' length exceeded the available height of the printing tray. Specimens 1-4 were tested after printing without further modification. Specimens 5-8 were covered with 4 layers of carbon fibre on each side after printing following the same procedure/orientation as the oil sump. The specimens' weight increased from 10 to 17 grams after the lay-up process.

Tensile tests were carried out using an Instron model 4505 (Instron Worldwide, Norwood, MA) tensile test machine that has a 200 kN load cell and is fitted with a long travel contact extensometer. Each sample was subjected to a cross-head speed of 1 mm/min until failure. The primary goal of the tensile testing was to generate force-extension data. To this end, a support computer connected to the tensile machine was used to visualize and record the force-extension curves of each of the specimens. With the stress-strain curve, the experimental elastic modulus was calculated in the linear region of the stress-strain curve. For specimens 1-4, the stress values at the strains of 0.005 and 0.015 were considered while for the specimens 5-8 the reference stresses were taken at 0.005 and 0.01. Figure 9 shows some specimens before and after testing.

Workbench testing

In order to analyse the new manufacturing approach presented in this paper, the physical prototype of the oil sump was tested with the help of a Suzuki combustion engine assembled to the FS car.

Two verification processes were performed. The first test was oriented to ensuring the correct fitting of the oil sump to the engine body in order to avoid any oil leaking through the joint itself or through the oil sump body by filtration. Hence, a liquid gasket was applied to the oil sump surfaces that are in contact to the engine body and, afterwards the sump was assembled to the engine with the help of the 14 tightening screws. Once dry, the liquid gasket should ensure the impermeability of the joint. Regarding the oil filtration through the sump, the density, number and orientation of the carbon fibre layers should solve the issue. Then, the engine was filled with oil and inspected to detect any oil droplets.

Afterwards, a second test was carried out where the prototype was subjected to a real scenario. The most critical moment for any element of a FS racing car is the Endurance event, where the reliability of the car is put to the test. In this event, the car has to complete 22 laps on a circuit that is slightly over 1km long. It takes around 30 minutes to complete the event, and the engine and the lubrication system are pushed to the limit, where the oil is at its nominal temperature and the oil pump is continuously and variably under operation. The test carried out in the workbench for this study tried to mimic the real competition conditions. In this way, the engine was started and the oil sump was tested for 45 minutes under realistic temperature conditions (80ºC). This test checked not only oil leaks but also possible deformations of the oil sump at nominal temperatures. The oil temperature was continuously monitored using the standard sensor of the Suzuki GSXR600 engine. The same is true for the oil pressure sensor. The oil pump speed is a direct function of engine speed. The engine speed, as measured in revolutions per minute (RPM), is not constant in a real situation. Analysing data from a real competition situation, the mean value for the engine speed is 8000 RPM. For this test, a safety factor of 1.2 was used, and the engine was operated at around 9.600 RPM during the test. The car's cooling system kept the oil at its nominal working temperature, slightly above 80ºC. In order to measure and record the temperature distribution in the oil sump during testing, a ThermaCAM P25 (Flir Systems, Wilsonville, Oregon, USA), which measures the infrared radiation of an object, was used. The camera was connected to a computer via USB, where the temperature distribution was monitored in real time. For a proper temperature measurement, the refraction index of the material was adjusted using a thermocouple as reference. After the test, the engine was stopped and left at rest for 3 weeks to detect any oil leakage. After the three weeks, it was disassembled and visually inspected.

Results

CFD results

The simulation results corresponding to the acceleration scenario with the old design is depicted in Figure 11. This simulation presented the most favourable scenario since the oil completely covered the base of the pick-up pipe for 5 seconds, and consequently, the oil pump was always fed with oil. The corresponding scenario with the new design was not simulated based on this last conclusion.

In the braking scenario, shown in Figure 12 and Figure 13, the oil moved forward, that is, it moved away from the pick-up point. The simulation of the old design showed that the oil pump started working without load at around 0.75 seconds while the oil movement was stabilized at 1.5 seconds. The new design was able to keep the oil close to the pick-up point until the 2-second mark, although the oil only was partially in contact to the base of the pick-up pipe from the 0.8 second mark.

In the lateral scenario (Figure 14 and Figure 15), the oil moved to one of the sides of the old oil sump and it got to a steady state at around 2 seconds. The pick-up pipe started being partially submerged in oil at 0.4 seconds, and from there on, the oil in contact to the pick-up pipe decreased as the simulation time increased. The new design increased the immersion time up to 0.8 seconds. After the 0.8 second mark, the pick-up pipe was not completely submerged.

Tensile testing

The stress-strain curves obtained for the different specimens are depicted in Figure 16. Just as a reminder, specimens 1 to 4 are simply ABS specimens obtained from the FDM process, and specimens 5 to 8 are ABS specimens from the FDM process but layered with carbon fibre. The results of the tensile tests are summarized in Table 2. With regard to Young's Modulus, the additive manufactured specimens averaged a value of 1491.2 MPa, with XZ being the strongest printing orientation. The specimens layered with carbon fibre presented a Young's Modulus that was around ten times higher. With respect to fracture stress, the behaviour was very similar since the carbon fibre provided almost seven times higher resistance. On the contrary, the results of elongation at break show that the ductility of the carbon fibre specimens was low: they broke without any warning at around 1.2 %.

Workbench testing

Results from testing indicated that the oil sump presented a good response. In the first test, it did not present any oil leak at ambient temperature. In a similar manner but with the engine running, the oil sump also presented good behaviour in terms of deformations and absence of leaks despite reaching temperatures close to 80ºC, very similar to the nominal oil temperature. Figure 17 represents a capture of the temperature distribution in one quarter of the oil sump external surface. Only this portion of the oil sump is shown as the temperature distribution was found to be practically symmetric with respect to the horizontal and vertical axes of the sump. This quarter of the oil sump is identified in Figure 7 by means of a white rectangle. The three lines represented in Figure 17 are used to measure the temperature in different directions, and the values are represented in Figure 18. It can be observed that the temperature is evenly distributed throughout the oil sump, with only 7ºC of difference between the centre and the edges. After this second test, the engine was stopped, and the oil sump was disassembled three weeks later. No failure in the inner surfaces of the oil sump was observed due to temperature.

Discussion

Several topics deserve further discussion, beginning with the computational simulations. As mentioned above, all the simulations were calculated by following the laminar flow condition and without considering any viscous models such as (k-ε) or (k-ω). D'Alessandro(D'Alessandro 2012) reviewed the state of the art for liquid sloshing in which he recaps several research projects and writes about both approaches. According to this recap, the majority of the works don't use any viscous models, but he also mentioned that the inclusion of the turbulence effect and their consequences in sloshing results is still under discussion among researchers. Assuming that the sloshing phenomenon is largely in viscid, we have assumed laminar flow as a good compromise between satisfactory results and simulation time. More precise simulations could be calculated in further works if necessary by considering standard turbulence models.

Another point of discussion is the oil height for the CFD simulations. In order to check the suitability of the new design against the worst scenario, we have assumed that the amount of oil in the sump is less than 0.6 litres (22mm height). Although this is not the real volume of oil presented in the oil sump while racing, it allowed us to check the suitability of the new wave-shape baffles more easily. Nevertheless, additional heights should be simulated to verify the appropriateness of the new baffles. According to the FS team, this height can be around 50 mm (1.5 litres of oil in volume). Additionally, it would be interesting to simulate the new design with simultaneous movements in various directions

With respect to the final functionality of the oil sump, we have to deal with two limitations that are not critical in the original oil sump. Firstly, the new design had to have reasonable mechanical behaviour without increasing the weight of the original design in aluminium. Secondly, it had to be impermeable to oil in order to avoid any leaking, since the nature of the FDM technology provides parts with porous structures. For the first limitation, one of the solutions could have been to directly print the oil sump in carbon fibre: the resulting prototype would have been stiffer than the ABS and the design freedom would not have been compromised. To the best of our knowledge, up to now, only SLS allows engineers to directly print in carbon fibre with the Nytek 1200 CF material. But as we do not have this material and printing technology at our facilities, we discarded it in our quest to follow the spirit of the Formula SAE competition. Regarding the FDM technology, the US Department of Energy (DOE) at Oak Ridge National Laboratory, among others, have demonstrated the possibility of 3D printing using carbon fibre, but the material is not yet available for sale. Nevertheless, although we had the carbon fibre feedstock for our FDM 3D printer, we still have had to face the second limitation: permeability due to the inherent deficiencies of the FDM process (parts are not oil-tight). For these reasons, we finally opted for Ilardo and Williams(2010) approach. The combination of the eight layers plus the resin allowed us to bypass both limitations since the carbon layers increased the base strength of the AM material, and the resin, which was pulled to the inside of the oil sump during the vacuum curing process, fixed the permeability issue once it was solid. For future work, it would be convenient to study if the number of carbon fibre layers could be reduced without compromising the permeability of the oil sump and its overall resistance to impacts from flying debris. This would mean a lighter and cheaper oil sump.

Following the same goal, a sump with a hollow, composite structure would be interesting to manufacture in order to analyse if just the carbon fibre layers could deal with those two limitations (Stratasys Ltd 2014). The idea would be to print the 3D model with soluble material, normally used for support structures, instead of the standard ABS plastic. After the composite lay-up process over the soluble core, the core would be dissolved in a support removal bath leaving a hollow carbon fibre sump. If we succeed, the sump would be extremely lighter. Nevertheless, this would not be a short term solution since our 3D printer cannot print in soluble material and we should hire an external company capable of printing with a Fortus AM machine.

Finally, another future approach could be testing the physical prototype presented in this paper on track. With the current testing outputs, it was demonstrated that the manufacturing process is valid and that the mechanical properties are good enough. However, the goodness of the new design in reducing the sloshing effect was only verified with virtual simulations. The goal of this stage would be to check the new design with simultaneous movements in various directions, that is, closer to realistic driving conditions. The idea would be to test the prototype under real world conditions with the upcoming 2015 car in order to verify that the simulations results are reasonable and that everything works properly. However, the realization of this idea presents a major handicap: how to validate the oil movement when in the car? In other sloshing studies, the validation procedure normally consists of building a Plexiglas mock-up that has various types of sensors to monitor pressures, temperatures, etc. The mock-up frame is normally transparent and at rest, so it is simple to visualize and validate the fluid movement. With our sump, the set-up is not so direct, and some possible solutions are still under discussion among the team. The short-term solution involves the assembly of the oil sump in the car while the driver regularly checks the pump pressure light indicator to see if the pump is properly working during the tests.

Conclusions

Several conclusions should be highlighted from this study. Despite the aforementioned limitations and assumptions, this paper presents a novel methodology for manufacturing oil sumps for motor vehicles by using FDM Additive Manufacturing technology in combination with a manual lay-up process with composite materials. Prior to fabrication, the oil sump was designed in CREO and simulated within the Fluent CFD application to verify the appropriateness of the new design in three sloshing scenarios. Simulation results indicated that the geometry of the new design showed better performance in comparison to the old oil sump made of aluminium in that the oil pick up-pipe was submerged in oil for more time. After fabrication, the sump was tested in a workbench where the prototype was assembled in a combustion engine. The engine was started and the oil sump was capable of withstanding an average temperature of 80ºC. Summing up, this work reaffirmed the possibility that the combination of Additive Manufacturing technologies and composite materials can be a real alternative to the conventional manufacturing processes of complex parts for competition automobiles.

References

Abramson, N. H. (1966). "Dynamic behaviour of liquids in moving containers." Scientic and Technical Information Division, National Aeronautics and Space Administration, Washington.

American Society for Testing and Materials International. (2012). "ASTM F2792 - 12a Standard Terminology for Additive Manufacturing Technologies."

Black, S. (2010). "Carbon fiber reinforced polyamide performs in engine part." Composites world magazine.

D'Alessandro, V., 2012. Modeling of a tank vehicle dynamics by fluid sloshing coupled simulation. Politecnico de Milano,

Dodge, F. T. (1971). "Engineering study of flexible baffles for slosh suppression."

Elsevier Ltd, 2013. Additive manufacturing helps racing team finish first. Metal Powder Report 68, 32-33.

Gibson, I., Rosen, D. W., and Stucker, B., 2010. Additive Manufacturing Technologies: Rapid Prototyping to Direct Digital Manufacturing. Springer,

Godderidge, B., Tang, M., Turnock, S., and Earl, C. (2006). "A verification and validation study of the application of computational fluid dynamics to the modelling of lateral sloshing." Ship Science Report No 140. University of Southampton.

Godderidge, B., Turnock, S., Tan, M., and Earl, C., 2009. An investigation of multiphase CFD modelling of a lateral sloshing tank. Computers & Fluids 38, 183-193.

Hirt, C. W., and Nichols, B. D., 1981. VOF method for the dynamics of free boundaries. Journal of Computational Physics 39, 201-225.

Ilardo, R., and Williams, C. B., 2010. Design and manufacture of a Formula SAE intake system using fused deposition modeling and fiber reinforced composite materials. Rapid Prototyping Journal 16, 174-179.

Lee, S.-H., Lee, Y.-G., and Jeong, K.-L., 2011. Numerical simulation of three-dimensional sloshing phenomena using a finite difference method with marker-density scheme. Ocean Engineering 38, 206-225.

Neugebauer, R., Müller, B., Gebauer, M., and Töppel, T., 2001. Additive manufacturing boosts efficiency of heat transfer components. Assembly Automation 31, 344-347.

Prada, J. G., Cazon, A., Carda, J., and Aseguinolaza, A., 2015. Direct Digital Manufacturing of an accelerator pedal for a Formula Student racing car. Rapid Prototyping Journal In Press,

Rhee, S. H., 2005. Unstructured Grid Based Reynolds-Averaged Navier-Stokes Method for Liquid Tank Sloshing. Journal of Fluids Engineering 127, 572-582.

SAE International. (2013). "2014 Formula SAE® Rules." Pages 163.

Spierings, A. B., Levy, G., Labhart, L., and Wegener, K., 2011. Production of functional parts using SLM – Opportunities and limitations. Proceedings of 5th International Conference on Innovative Developments in Virtual and Physical Prototyping, Leira (Portugal).

Stephens, D. G., and Scholl, H. F. (1967). "Effectiveness of Flexible and Rigid Ring Baffles for Damping Liquid Oscillations in Large-Scale Cylindrical Tanks." Washington D.C, USA. .

Stratasys Ltd. (2014). "FDM sacrifial cores and mandrels for composite layups."

Tables

Specimen	Orientation	Carbon Fibre
1	XY	-
2	XZ	-
3	YX	-
4	YZ	-
5	XY	Yes
6	XZ	Yes
7	YX	Yes
8	YZ	Yes

Table 1 The 8 specimens according to the printing orientation and the presence of carbon fibre layers

Specimen	Elongation at break (%)	Fracture stress (MPa)	E modulus (MPa)
1	4	24.8	1312
2	7.3	26	1749
3	8.3	24.5	1409
4	5.2	26	1495
Average	6.2	25.32	1491.25
5	1.1	170	15653
6	1.15	178	15234
7	1.2	180	15417
8	1.35	190	13953
Average	1.2	179.5	15064

Table 2 Tensile testing result for the 8 specimens according to the printing orientation and the presence of carbon fibre layers

Figure Captions

Figure 1 Original oil sump of the FS2013 car: virtual model (left) and physical component (right)

Figure 2 New design for the oil sump: overview of the virtual model (left) and a detailed view of the baffles (right)

Figure 3 Engine ready for scanning (left) and detail of the pick-up pipe (right)

Figure 4 Final control volume: bottom view for the old (left) and new (centre) design and top view for both designs (right)

Figure 5 Initial time for the CFD simulation: old sump (left) and new sump (right)

Figure 6 New design for the oil sump: Partition lines with connector pins and with reference axis showing the printing orientation (left) and the physical prototype once all the parts are printed and glued, with an axis showing the longitudinal axis of the vehicle to have a reference for the assembly of the sump (right)

Figure 7 New oil sump after the lay-up process with carbon fibre

Figure 8 Specimen dimensions in mm for tensile testing

Figure 9. ABS specimen ready for testing (a), the same specimen once broken (b), a layered specimen after testing (c) and a detailed view of the rupture point (d)

Figure 10 Suzuki GSRX 600 engine place in the FS vehicle with the oil sump assembled (left) and the ThermaCAM P25 ready to measure temperature distribution during the test (right).

Figure 11 Cross-sectional view showing the oil sloshing in the old design during acceleration (0-1.5s). Images were taken every 300 milliseconds.

Figure 12 Cross-sectional view of the oil sloshing in the old design during braking (0-2s). Images were taken every 400 milliseconds.

Figure 13 Cross-sectional view of the oil sloshing in the new design during braking (0-2s). Images were taken every 400 milliseconds.

Figure 14 Cross-sectional view of the oil sloshing in the old design during lateral movement (0-2s). Images were taken every 400 milliseconds

Figure 15 Cross-sectional view of the oil sloshing in the new design during lateral movement (0-2s). Images were taken every 400 milliseconds

Figure 16 Stress-strain curves for the 8 specimens: specimens 1-4 (left) and 5-8 (right)

Figure 17 Temperature distribution as recorded using the ThermoCAM P25. The region with the lowest temperatures in black (top left) represents the surface temperature of a sensor used by the camera as reference, and should not be considered when analysing the results

Figure 18 Temperature values throughout the length of the lines represented in Figure 17

Response to Reviewer #1

Following is the response to the reviewer's comments concerning our paper NVPP-2015-0017 entitled "Pilot study describing the design process of an oil sump for a competition vehicle by combining Additive Manufacturing and carbon fibre layers." by Aitor Cazón, Jorge G. Prada, Eric García, Gorka S. Larraona and Sergio Ausejo. We thank the reviewer for his/her comments on our paper, which have allowed us to improve the manuscript in this revision.

This paper reported a design process of an oil sump using additive manufacturing and carbon fibre layers. A relative cheap and high performance composite oil sump has been fabricated successfully. Various methods including CFD and tensile test have been applied to provide further design theory and performance verification. It is a very well written paper with many in-depth discussions.

Thank you for the positive feedback.

Page 5 line 31, change "my" to "by"

Thank you for the comment. We have corrected the typo.

Page 10, line 22-29, the two equations are not necessary. They are very well known.

We do completely agree with this appreciation, so we have eliminated those equations.

Page 14. Line 37. " but as we do not have this material…" just a comment here. I don't think it will work even you have the Nytek 1200 CF materials. Most of the SLS printed parts are porous as well so it is likely that there will be leakage if you SLS printed it without any post treatment for impermeable surface.

Thank you very much for pointing this out. We were not aware of that fact, probably because we are not familiarized with technology.

Response to Reviewer #2

Following is the response to the reviewer's comments concerning our paper NVPP-2015-0017 entitled "Pilot study describing the design process of an oil sump for a competition vehicle by combining Additive Manufacturing and carbon fibre layers." by Aitor Cazón, Jorge G. Prada, Eric García, Gorka S. Larraona and Sergio Ausejo. We thank the reviewer for his/her comments on our paper, which have allowed us to improve the manuscript in this revision.

The paper present interesting work done by students who are passionate and dedicated to the pursuit of the FS challenges. This is an innovative process to produce high strength light weight components which will be of interest to other teams of students. Under the circumstance of limited resources they have done good work.

Thank you for the positive feedback.

Page 5, line 55 remove 'welding' which is not a subtractive process

The reviewer is completely right, so we have removed that process and rearranged the text.

(Page 5, line 55): milling or drilling.

Page 10, line 46, a figure to correlate the direction of printing and the specimen longitudinal (test) direction is required to explain this.

Some extra information has been added to Figure 6 and its caption trying to solve this aspect.

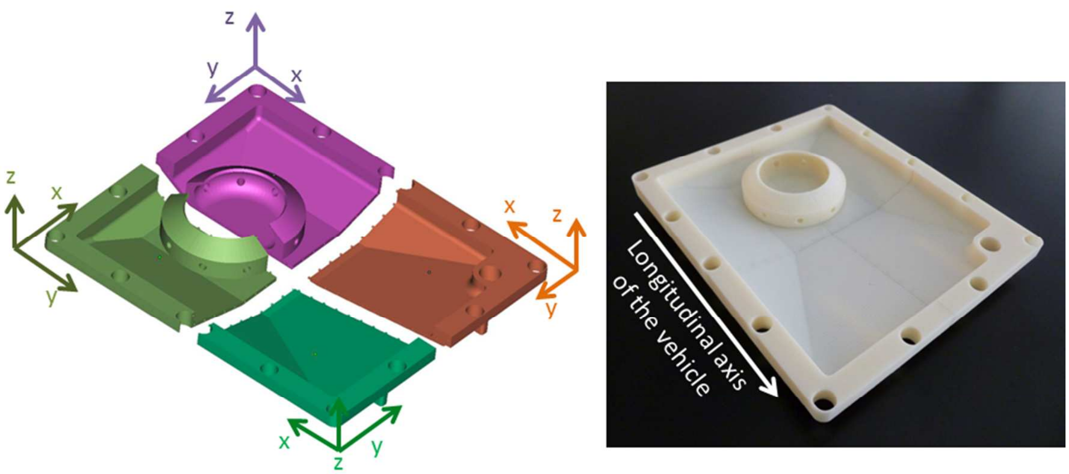

Figure 6 New design for the oil sump: Partition lines with connector pins and with reference axis showing the printing orientation (left) and the physical prototype once all the parts are printed and glued, with an axis showing the longitudinal axis of the vehicle to have a reference for the assembly of the sump (right)

Also good to show photographs of the test specimens before and after tensile tests. the failure modes of the samples should be elaborated to show understanding of the failure modes.

Thank you for this comment. We have added a new sentence in the "Methods. Tensile Testing" section related to this topic and a picture for illustration.

(Page 10, Line 21) Figure 9 shows some specimens before and after testing.

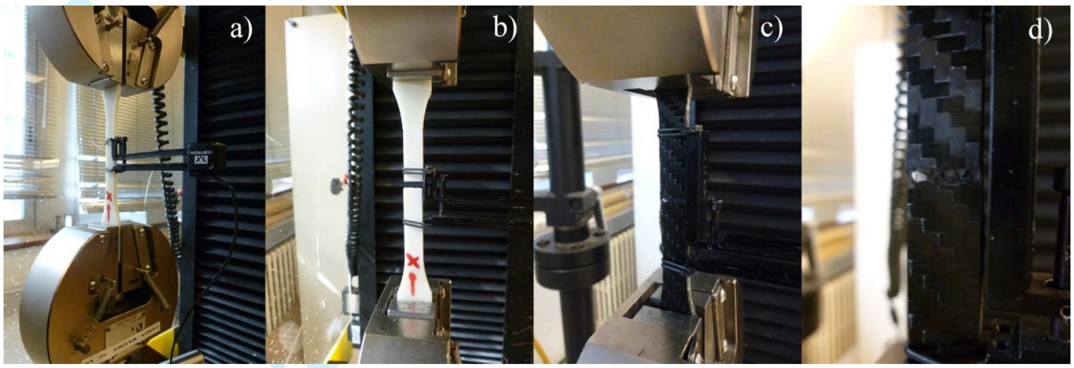

Figure 9. ABS specimen ready for testing (a), the same specimen once broken (b), a layered specimen after testing (c) and a detailed view of the rupture point (d)

Stress strain plots for tensile tests should be plotted out. These are standard requirement of showing tensile test results.

(Page 12, Line 26) The stress-strain curves obtained for the different specimens are depicted in Figure 16. Just as a reminder, specimens 1 to 4 are simply ABS specimens obtained from the FDM process, and specimens 5 to 8 are ABS specimens from the FDM process but layered with carbon fibre.

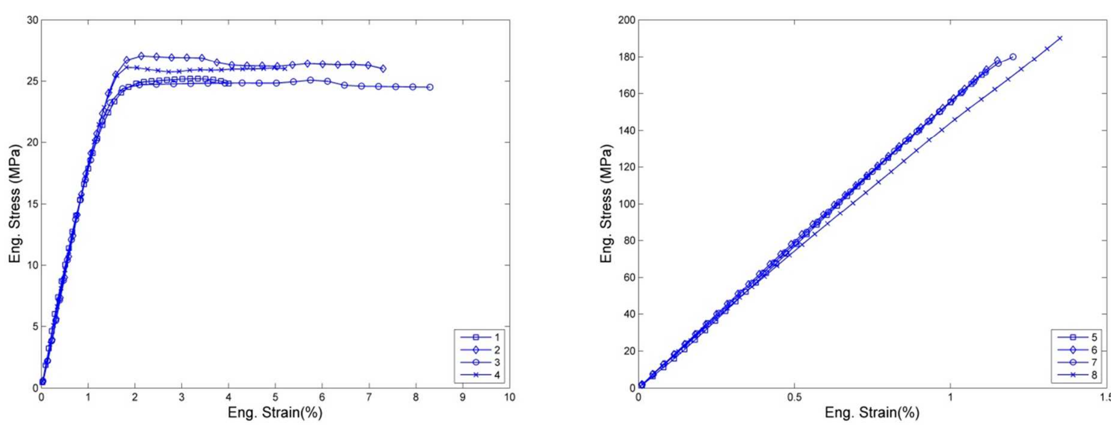

Figure 16. Stress-strain curves for the 8 specimens: specimens 1-4 (left) and 5-8 (right)

How does the surface roughness of the printed surfaces affect adhesion to carbon fabric? At what resolution are the parts printed at and how do you know that the carbon cloth or resin adhere will adhere well to the ABS plastic surface? Any tests (such as peel test) conducted?

No tests have been carried out in this sense. It is true that such test would help to completely understand the issue and the process here addressed, but we did not find it necessary for three main reasons:

1. *Some of the FDM technology manufacturers (Stratasys, http://www.cimetrixsolutions.com/downloads/AG-CarbonFiber.pdf) claim FDM to "have compelling reasons for using it instead of other additive fabrication technologies… the inherent porosity of FDM parts aids in adhesion". The same resin that provides the stiffness for the carbon fibre cloth is also the bonding agent for the union between the core and the carbon fibre layers.*
2. *Some other studies have already used carbon fibre layered upon FDM parts, with satisfactory result (Ryan Ilardo, Christopher B. Williams, (2010) "Design and manufacture of a Formula SAE intake system using fused deposition modeling and fiber-reinforced composite materials", Rapid Prototyping Journal, Vol. 16 Iss: 3, pp.174 – 179)*
3. *The test carried out and described in the workbench section, although is not particular for peeling studies, can also be used to determine whether there will be peel problems or not, the results being satisfactory in this case.*

Page 11, line 48 The temperature distribution shown in the figure should be identified with the orientation of the sump bottom.

Some extra information has been added to figure 7 trying to solve this aspect.

(Page 11, line 11) This quarter of the oil sump is identified in Figure 7 by means of a white rectangle.

Figure 7 New oil sump after the lay-up process with carbon fibre

Page 11, line 55 After 3 weeks, if oil has seeped through the carbon into the ABS below, how can that be detected? Have any tests being done to determine the resin's resistance to prolonged oil immersion?

We are aware of two ways to check this:

1. *One would be using destructive methods, inspecting the inside of the part in several sections. As we have created only one prototype and we want to use it when racing, those tests cannot be conducted.*
2. *The other one is using a weighing scale before and after the test: the weight of the part was the same in our case, so it can be concluded that there is no oil has broken in.*

Page 15, line 17 should be "dissolved".

Thank you for pointing out. Correction done.

General improvements in clarity are needed as listed below:
1. Figures are too small or low in resolution

We are sorry about that. The original images are too heavy for the online submission application, so we had to reduce them: it seems we have gone from one extreme to the other. We will provide proper quality and size images this time.

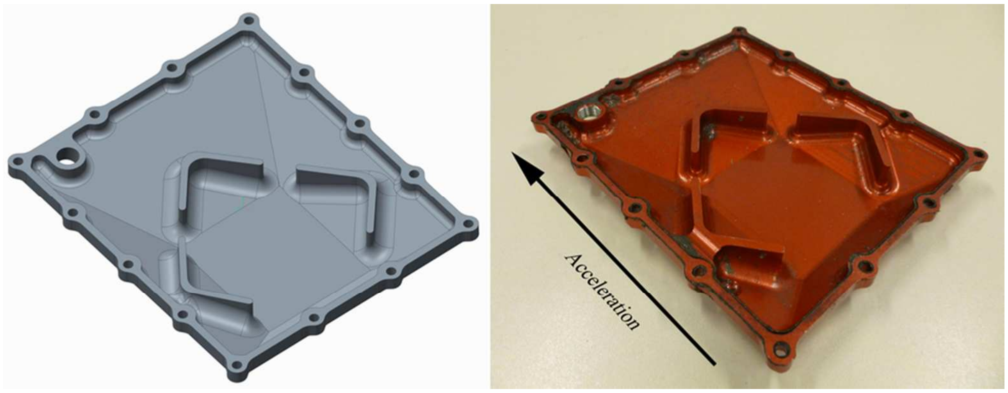

Original oil sump of the FS2013 car: virtual model (left) and physical component (right)
40x15mm (600 x 600 DPI)

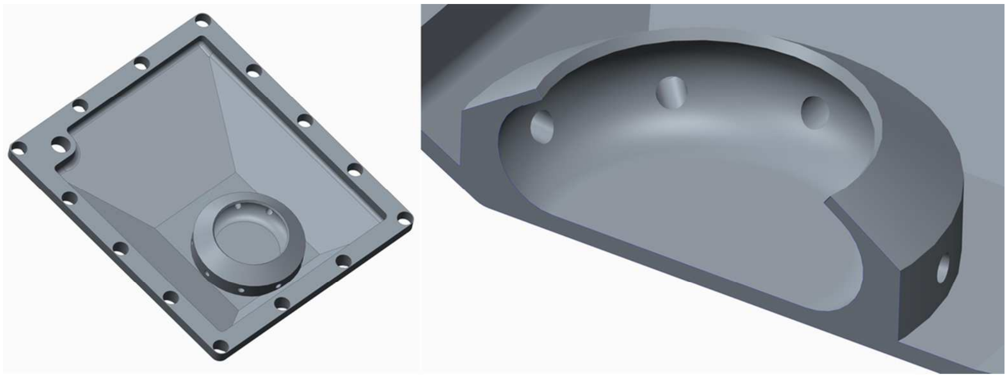

New design for the oil sump: overview of the virtual model (left) and a detailed view of the baffles (right)
49x18mm (600 x 600 DPI)

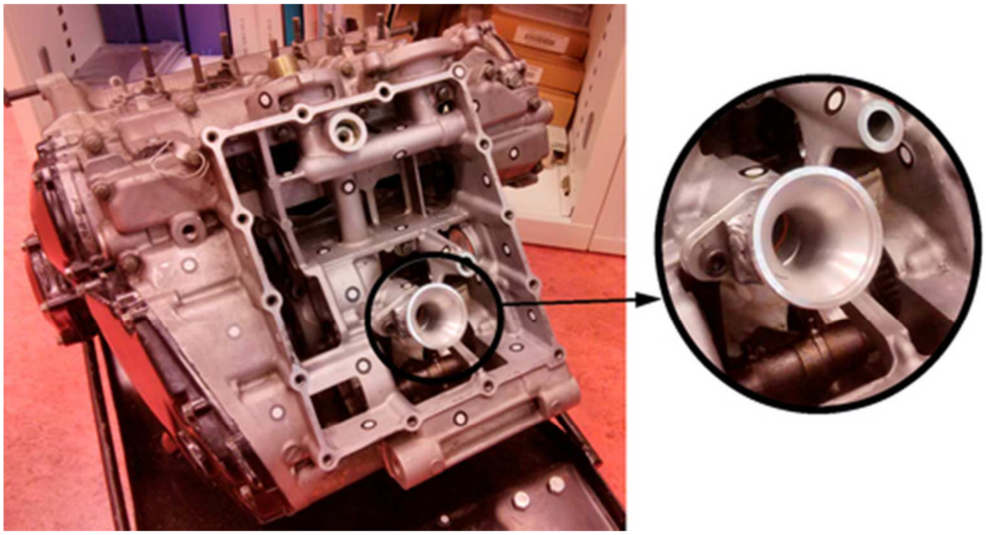

Engine ready for scanning (left) and detail of the pick-up pipe (right)
21x11mm (600 x 600 DPI)

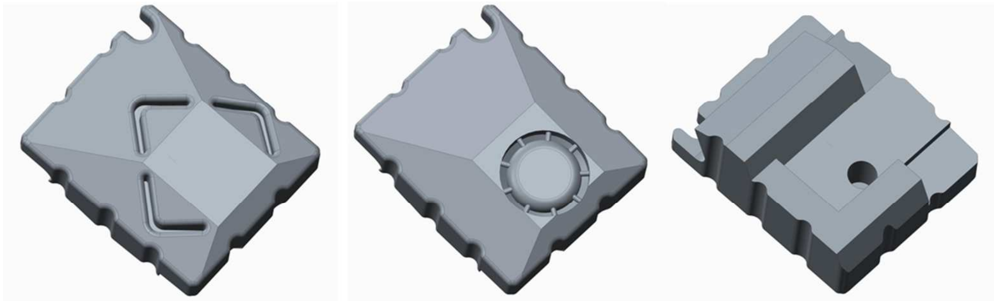

Final control volume: bottom view for the old (left) and new (centre) design and top view for both designs (right)
45x13mm (600 x 600 DPI)

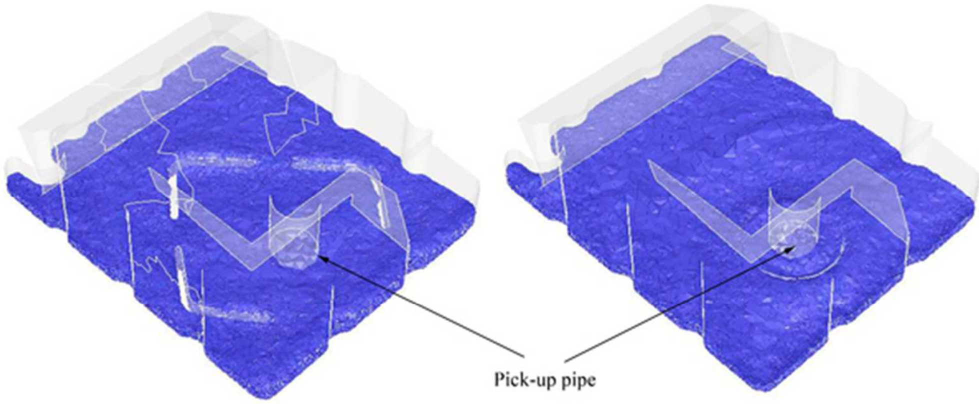

Initial time for the CFD simulation: old sump (left) and new sump (right)
25x10mm (600 x 600 DPI)

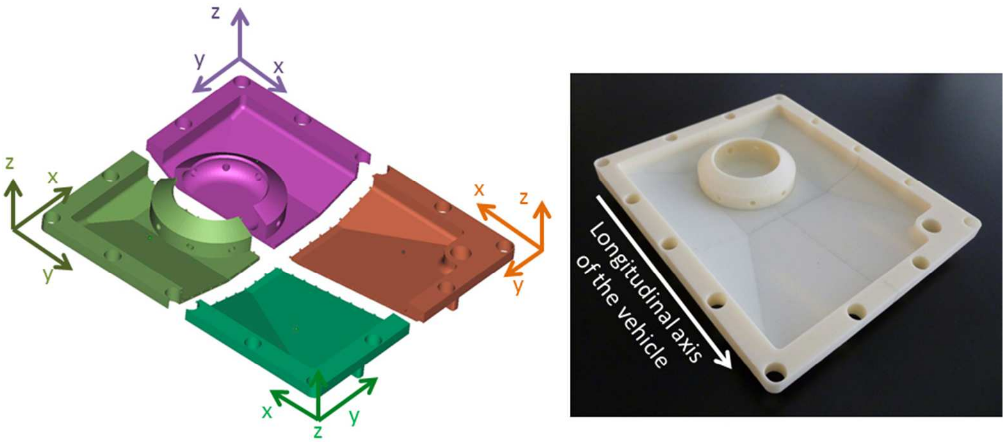

New design for the oil sump: Partition lines with connector pins and with reference axis showing the printing orientation (left) and the physical prototype once all the parts are printed and glued, with an axis showing the longitudinal axis of the vehicle to have a reference for the assembly of the sump (right)
253x115mm (96 x 96 DPI)

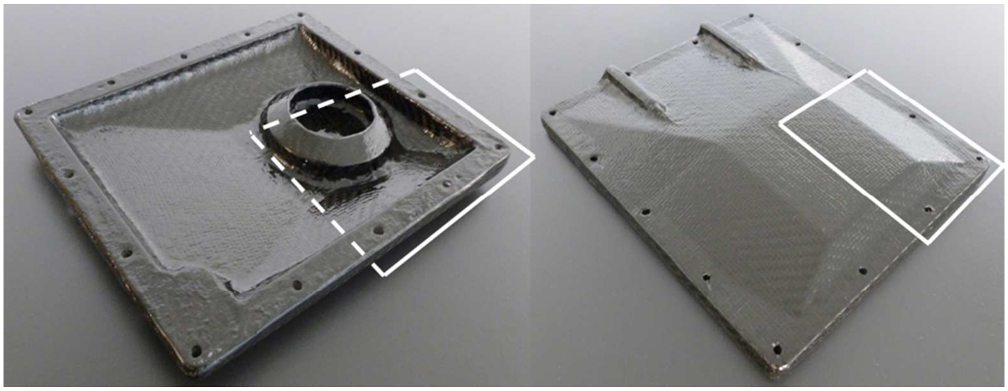

New oil sump after the lay-up process with carbon fibre
253x96mm (96 x 96 DPI)

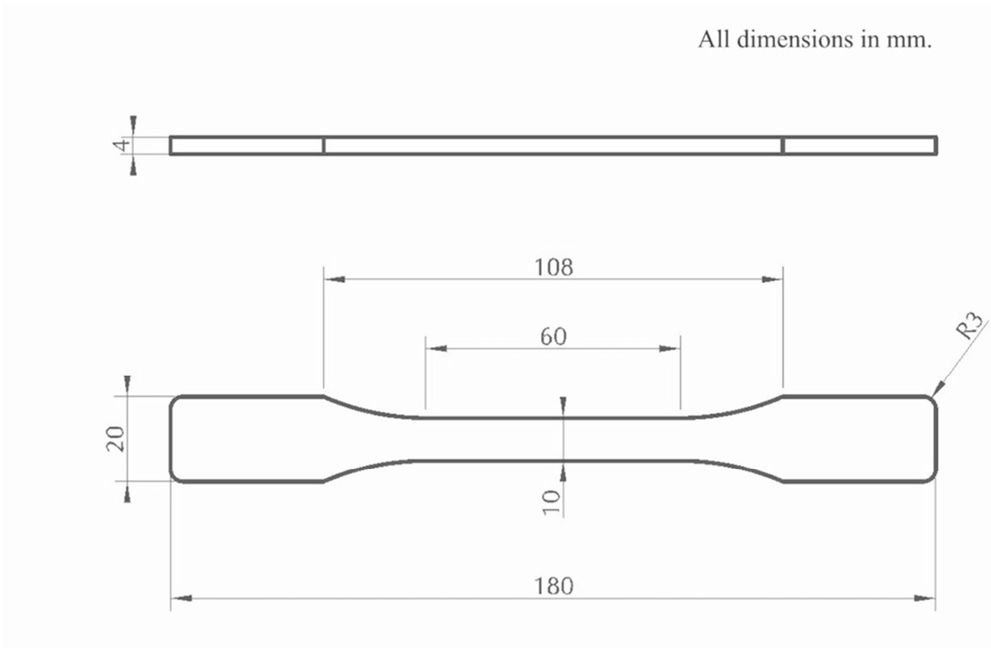

Specimen dimensions in mm for tensile testing
45x29mm (600 x 600 DPI)

Specimen	Orientation	Carbon Fibre
1	XY	-
2	XZ	-
3	YX	-
4	YZ	-
5	XY	Yes
6	XZ	Yes
7	YX	Yes
8	YZ	Yes

Table 1 The 8 specimens according to the printing orientation and the presence of carbon fibre layers

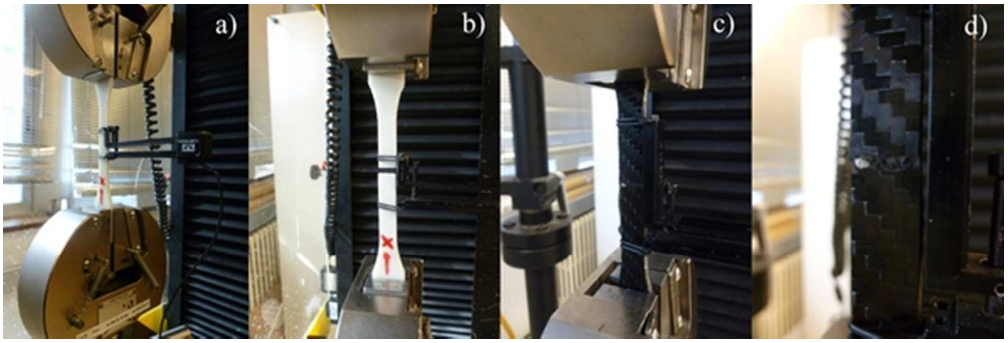

ABS specimen ready for testing (a), the same specimen once broken (b), a layered specimen after testing (c) and a detailed view of the rupture point (d)
25x8mm (600 x 600 DPI)

Suzuki GSRX 600 engine place in the FS vehicle with the oil sump assembled (left) and the ThermaCAM P25 ready to measure temperature distribution during the test (right).
150x49mm (300 x 300 DPI)

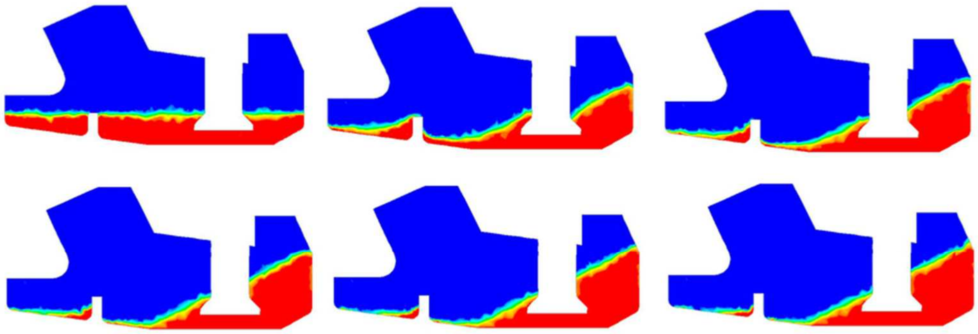

Cross-sectional view showing the oil sloshing in the old design during acceleration (0-1.5s). Images were taken every 300 milliseconds.
37x13mm (600 x 600 DPI)

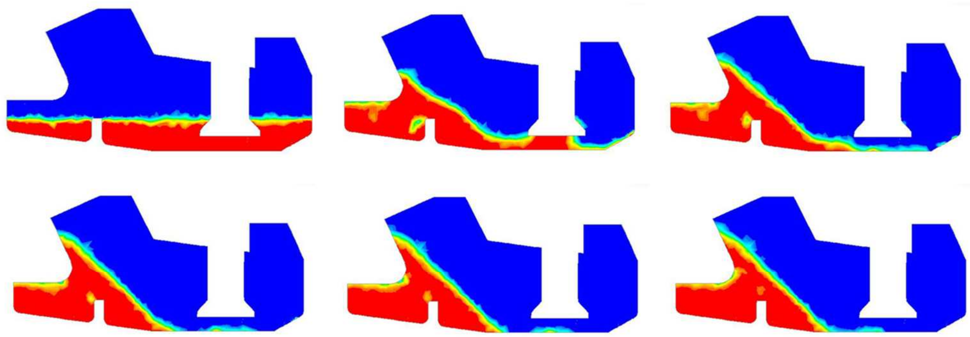

Cross-sectional view of the oil sloshing in the old design during braking (0-2s). Images were taken every 400 milliseconds.
56x21mm (600 x 600 DPI)

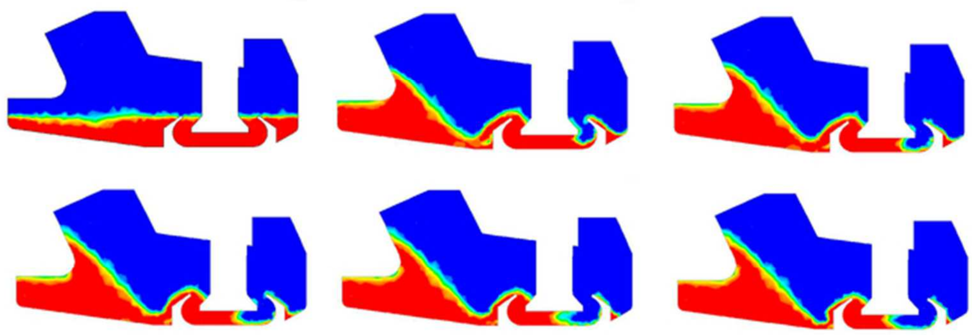

Cross-sectional view of the oil sloshing in the new design during braking (0-2s). Images were taken every 400 milliseconds.
28x10mm (600 x 600 DPI)

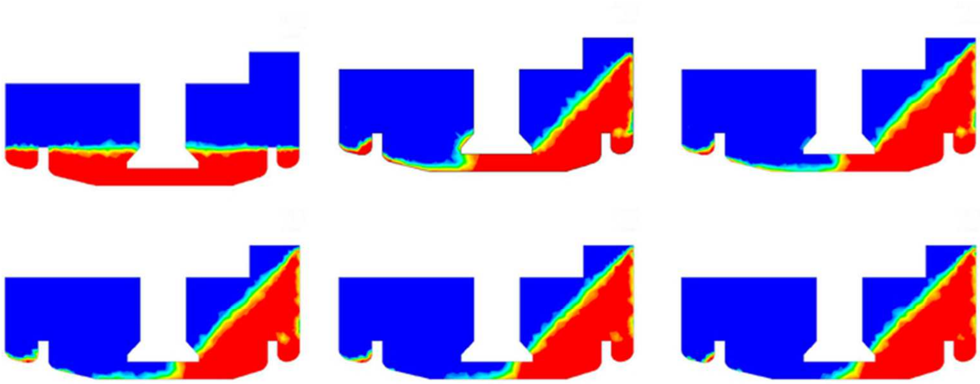

Cross-sectional view of the oil sloshing in the old design during lateral movement (0-2s). Images were taken every 400 milliseconds
30x12mm (600 x 600 DPI)

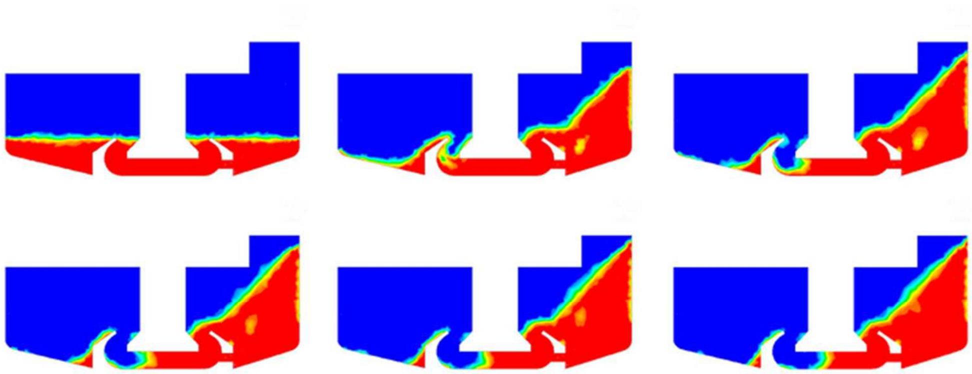

Cross-sectional view of the oil sloshing in the new design during lateral movement (0-2s). Images were taken every 400 milliseconds
30x12mm (600 x 600 DPI)

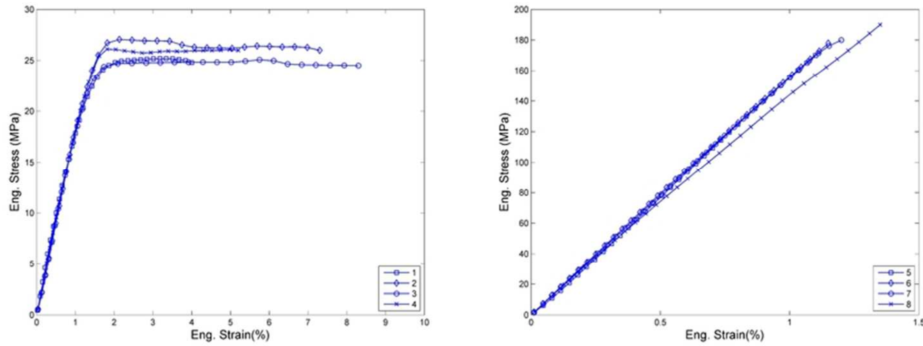

Stress-strain curves for the 8 specimens: specimens 1-4 (left) and 5-8 (right)
76x28mm (300 x 300 DPI)

Specimen	Elongation at break (%)	Fracture stress (MPa)	E modulus (MPa)
1	4	24.8	1312
2	7.3	26	1749
3	8.3	24.5	1409
4	5.2	26	1495
Average	6.2	25.32	1491.25
5	1.1	170	15653
6	1.15	178	15234
7	1.2	180	15417
8	1.35	190	13953
Average	1.2	179.5	15064

Table 1 Tensile testing result for the 8 specimens according to the printing orientation and the presence of carbon fibre layers

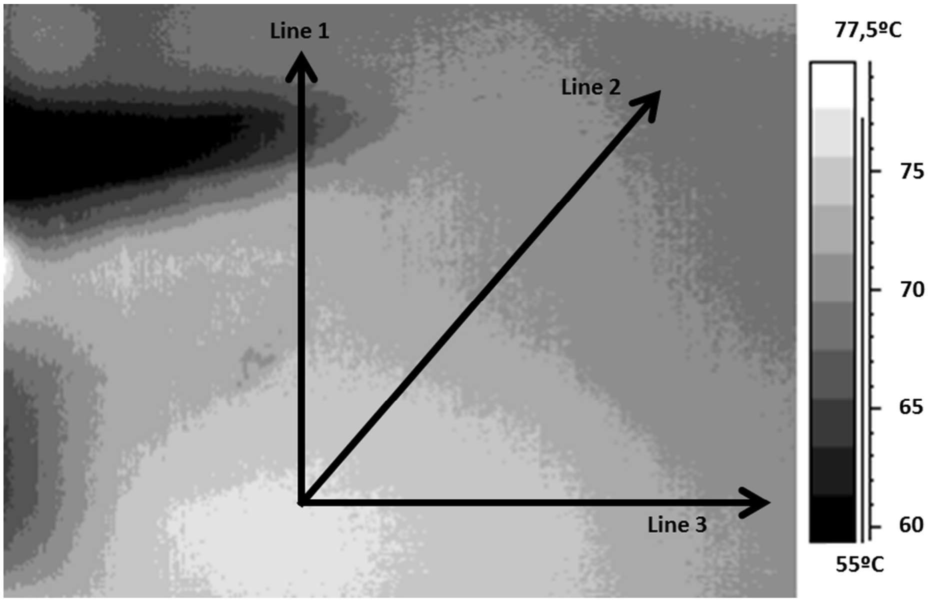

Temperature distribution as recorded using the ThermoCAM P25. The region with the lowest temperatures in black (top left) represents the surface temperature of a sensor used by the camera as reference, and should not be considered when analysing the results
150x89mm (300 x 300 DPI)

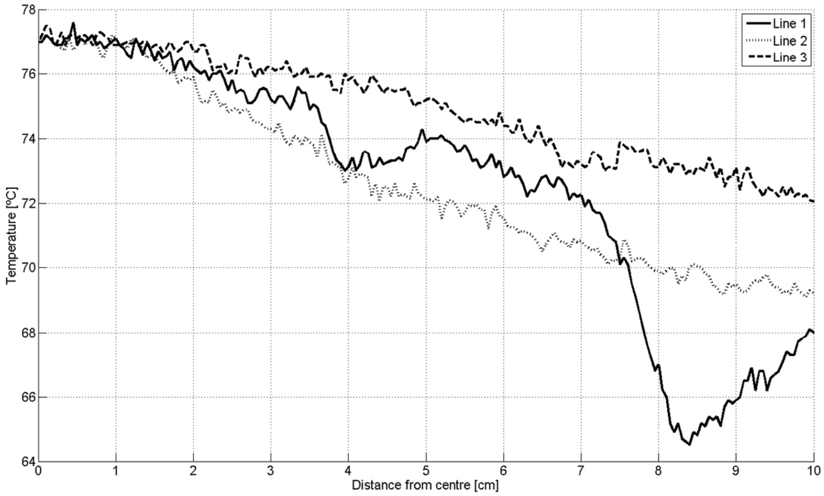

Temperature values throughout the length of the lines represented in Figure 17
150x83mm (300 x 300 DPI)